

Universitat de Lleida

Document downloaded from:

<http://hdl.handle.net/10459.1/59369>

The final publication is available at:

<https://doi.org/10.1007/s11829-016-9425-0>

Copyright

(c) Springer Science+Business Media Dordrecht, 2016

1 **Analysing spatial correlation of weeds and harvester ants in cereal fields using**
2 **point processes**

3

4 Running title: Spatial correlation of weeds and harvester ants

5

6 Carles Comas¹, Aritz Royo-Esnaol², Jordi Recasens², Joel Torra*²

7 ¹Department of Mathematics, AGROTECNIO, Universitat de Lleida, Avda. de l'Estudi General,
8 4 E-25001, Lleida, Spain.

9 ²Weed Science and Plant Ecology Research Group, Department of Hortofructicultura, Botànica
10 i Jardineria, AGROTECNIO, ETSEA, Universitat de Lleida, Avda. Rovira Roure 191, E-25198
11 Spain.

12 * Corresponding author. Email address: joel@hbj.udl.cat; tel. No. +34973702318; fax. No.
13 +34973238264

14

15

16

17

18

19

20

21

22

23

24

25

26

27

28 **Abstract**

29 The interaction between the spatial distribution of weed richness and weed cover and the spatial
30 location of harvester ant nests was investigated in cereal fields. The understanding of such
31 interdependencies can be relevant to understand weed population dynamics in dryland cereal
32 fields and may enhance management strategies for weed control. We used spatial statistical
33 tools derived from point process theory. In particular, we compared the two spatial
34 configurations by assuming two different point patterns. We did so by replacing the weed
35 random fields by a related point pattern and comparing it with the point pattern of harvester
36 ants. Our results suggest that areas with a high density of ant nests are in general areas with low
37 weed richness and low weed cover, and that large nests have a greater impact on weed spatial
38 configurations than small nests. Thus preserving and enhancing regular ant nest distributions,
39 especially of large nests, would have a major impact on depleting weed density and
40 consequently enhancing weed control.

41

42 **Keywords** Cross-pair correlation function, *Messor barbarus*, Point pattern, Random field,
43 Weed plants.

44

45

46

47

48

49

50

51

52

53

54

55

56 **Introduction**

57

58 Weed species are distributed unevenly in arable fields and, consequently, diversity is not
59 expected to be homogeneous within the fields (Izquierdo et al. 2009a). Weeds occur in patches
60 because they tend to cluster where conditions favour propagule banks and seed dispersal
61 (Colbach et al. 2000). Biotic, abiotic, and anthropogenic processes likely contribute to the
62 expression of weed “patchiness” in agricultural fields (Williams et al. 2002). The spatial
63 distribution may be related to the interaction of several of these factors, such as soil type (
64 Burton et al. 2006; Di Virgilio et al. 2007; Dieleman et al. 2000), cultivation or tillage (Barroso
65 et al. 2006; Burton et al. 2006; Colbach et al. 2000; Heijting et al. 2009), harvesting (Barroso et
66 al. 2006; Blanco-Moreno et al. 2004; Heijting et al. 2009), herbicides (Barroso et al. 2004;
67 Dieleman et al. 2000) and competition between crop and weeds (Blanco-Moreno et al. 2006).
68 Spatially explicit factors affecting seed distribution, germination and survival have a big impact
69 on weed spatial distribution and dynamics (Blanco-Moreno et al. 2004). However, differences
70 in weed population dynamics and spatial distribution with respect to within-field heterogeneity
71 are not well documented despite increasing interest in site-specific management of agro-
72 ecosystems (Burton et al. 2006). Moreover, the evaluation of the spatial structure of weed
73 diversity and factors that determine it (i.e. field management or landscape heterogeneity) can be
74 extremely important in biodiversity studies (Izquierdo et al. 2009a). Finally, the understanding
75 of spatial dynamics of weed patches is of fundamental importance for achieving realistic models
76 of weed populations and for weed management (Blanco-Moreno et al. 2006).

77 Several reasons for weed patchiness have been proposed, but it is clear that the factors
78 that influence weed mortality are among the most important (Dieleman and Mortensen 1999;
79 Woolcock and Cousens 2000). One of the factors that is known to have a big impact on weed
80 survival and population dynamics is epigeaic seed predation (Westerman et al. 2003). In dryland
81 cereals of NE Spain the main seed predator is the harvester ant *Messor barbarus* L. (Baraibar et
82 al. 2009). This species causes 46%-100% of post-dispersal seed losses before weed seeds enter
83 the seedbank (Westerman et al. 2012). Harvester ants can cause significant losses of weed seeds

84 in dryland cereals and can thus contributing to weed control (Baraibar et al. 2011). However,
85 harvester ant nests are not evenly distributed on the field (Díaz 1992), because factors such as
86 soil characteristics (Wiernasz and Cole 1995), field management (Díaz 1991) and interaction
87 between nests (Ryti and Case 1992) affect these distribution patterns. A previous study in NE
88 Spain indicated that the origin of spatial trends (4-12 m) of harvester ants in cereal fields should
89 be sought in biotic factors, such as seed availability or intrinsic ones (Blanco-Moreno et al.
90 2014). Because harvester ant abundances are not constant in fields, seed predation rates are not
91 equal within a dryland cereal field (Torra et al. in press). Therefore, if there is spatial variability
92 in the seed predation by harvester ants, we hypothesize that there can also be a spatial
93 relationship between this process and the spatial distribution of weeds in these cereal fields.
94 This could partially explain the spatial and temporal dynamics of weeds and seed losses in the
95 life cycle of annual weeds highlighted by Dicke et al. (2007), at least in the study area.

96 This paper analyses the interaction between the spatial distribution of weeds and the
97 spatial location of ant nests. In particular, it considers weed richness and weed cover samples
98 over a rectangular grid, and the spatial location and size of ant nests. These two sampling
99 processes result in two different sets of spatial data, i.e. point referenced data (lattice) for the
100 weed samples and a point pattern for the ant nests (Cressie 1993). Since the pioneering paper of
101 Ford (1975), who studied the effect of between-plant competition on *Tagetes patula* L.
102 (marigolds) planted on a regular grid, several studies have used lattice data to analyse the spatial
103 distribution of plants, including the spatial and temporal structures of weeds (Barroso et al.
104 2004; Blanco-Moreno et al. 2006; Colbach et al. 2000; Izquierdo et al. 2009a). The spatial
105 analysis of ant nests has also been investigated by regarding their nests as a point pattern (see
106 among others, Harkness and Isham 1983; Nicolai et al. 2010; Tanner and Keller 2012), also in
107 cereal fields (Blanco-Moreno et al. 2014). A spatial point process is a stochastic mechanism that
108 generates a countable set of events x_i in a bounded region A (see, for instance, Diggle 2003); a
109 point pattern is a stochastic realization of a point process. Animal and plant ecology has applied
110 numerous statistical methods belonging to point processes (Diggle 2003; Illian et al. 2008;

111 Stoyan and Penttinen 2000; Wiegand et al. 2006) to tackle ecological management questions
112 (Comas 2009; Comas and Mateu 2011; Law et al. 2009). However, few approaches (if any)
113 have combined both sets of sample data to analyse the interaction between spatial structures of
114 weeds and ants. The analysis of these interactions may be valuable for interpreting the processes
115 governing the spatial relationship between weed plants and harvester ants, thus providing key
116 information on the life cycle for future control management of weed species in cereal fields.

117 The main objective of this study was to investigate the spatial interdependencies
118 between spatial locations of harvester ant nests and the spatial configuration of weed richness
119 and coverage. To do so we considered a novel methodology based on spatial statistical tools
120 derived from point process theory. To the best of our knowledge this the first time that the space
121 spatial structure of weeds and ants are analysed using point processes.

122

123 **Materials and Methods**

124

125 Study area

126 A no-tillage dryland cereal field was surveyed to analyse the relationship between the spatial
127 distribution of its weeds and harvester ant nests. The selected field (2 ha), located in Bellmunt
128 d'Urgell, Spain, was managed following the usual practices of the region. Barley was sown at a
129 rate of 180 kg/ha in late October. Broad-leaved weeds were controlled with a mixture of
130 herbicides (florasulam + 2,4-D at 0.75 l/ha) on 10 March 2011.

131

132 Data

133 Weed species and abundance were evaluated in early May 2011 after herbicide spraying. The
134 percentage of total weed cover and the number of species were recorded in 50 x 50 cm quadrats
135 located every 10 m in a 150 x 50 m grid placed on the field, resulting in 96 sampling units. In
136 each quadrat, weed cover of each species was determined using a scale from 0 to 100. Nodes
137 were georeferenced using a differential global positioning system (DGPS), model GS02, with
138 centimetre precision (Leica Geosystems AG, Heerbrugg, Switzerland). Moreover, *Messor*

139 *barbarus* nest abundance and spatial distribution was recorded in the experimental area in early
140 August 2011 after harvest. In this case, we recorded nest abundance in a 50 x 50 m small region
141 of the rectangular area where weed species and abundance were evaluated. The nests were
142 usually determined by counting one opening per nest, though large nests were assumed to have
143 more than one entrance. Nests were only included if ants were detected, to prevent counting of
144 abandoned nests. Therefore, counting was done from sunrise until around noon, because high
145 temperatures limit ant activity (Azcárate et al. 2007). All nests were marked with spray-paint to
146 prevent double counting, and nest size was determined using a subjective scale ranging from 1
147 (smallest) to 5 (largest), according to the area occupied by the colony, the number of entrances,
148 worker size and the number of active ants (Baraibar et al. 2011). This classification is based on
149 the assumption that larger colonies will have more reproductive adults and that there will be
150 more openings for their release. Four nest sizes were therefore classified into four main
151 categories: categories 1 and 2 for nest sizes $<0.4 \text{ m}^2$; category 3 for nest sizes in the range $0.4\text{-}1$
152 m^2 ; category 4 for nest sizes in the range $1\text{-}2 \text{ m}^2$; and category 5 for nest sizes $>2 \text{ m}^2$. This
153 classification distinguishes between nests with a single entrance (category 1) and nests with
154 more than one entrance (categories 2, 3, 4 and 5) (Baraibar et al. 2011). Finally, each marked
155 nest was georeferenced with the DGPS mentioned above.

156

157 Spatial statistics

158 *Analysing the spatial point structure of ant nests*

159 The spatial structure of a point pattern can be described by various summary characteristics. To
160 analyse the spatial structure of ant nests (point locations) we used a spatial correlation function
161 derived from point process theory. We considered the pair correlation function (Illian et al.
162 2008), an estimator of which can be obtained as

163

$$164 \hat{g}(r) = \frac{1}{2\pi\hat{\lambda}^2|A|} \sum_{(x_1, x_2) \in \phi}^{\neq} \frac{\kappa(\|x_1 - x_2\| - r)}{e(x_1, \|x_1 - x_2\|)} \quad (1)$$

165

166 for a given observation region A with area $|A|$ and inter-point distance r . Here φ is the
167 observed point pattern, $\hat{\lambda}$ is an estimator of the point intensity, i.e. the number of points (i.e.
168 nests) per unit space, $\kappa(\cdot)$ is the Epanechnikov kernel function, \sum^{\neq} stands for the summation
169 over all pairs such that $x_i \neq x_j$, where $x_i = \{x_{i1}, x_{i2}\}$ is a point in the Euclidian plane, and $e(\cdot)$
170 is the Ripley's factor (Ripley 1976) to correct edge effects. Broadly speaking, this function
171 indicates point inhibition when $\hat{g}(r) < 1$, $\hat{g}(r) = 1$ denotes the Poisson case (i.e. a random point
172 process) with no interaction between points, while $\hat{g}(r) > 1$ implies point clustering for any
173 $r > 0$.

174

175 *Analysing the spatial dependence between ant nets and weed richness and coverage weeds*
176 *based on point process correlation functions*

177 To analyse the spatial dependences between the distribution of ant nests and the spatial
178 configuration of weed richness and coverage, we used spatial statistical tools derived from point
179 process theory. In particular, we adopted an approach initially formulated by Illian et al. (2008)
180 to analyse the spatial correlation between point patterns and random fields. This statistical
181 approach is based on comparing some summary statistics associated with these spatial
182 structures. Consider a stationary and isotropic space point process Φ in two dimensions with
183 point intensity λ and a random field $Z = Z(x)$, where x is any location in the Euclidian plane,
184 both processes over an observation window A (i.e. the area of study). The basic idea of this
185 approach is to replace Z by a point pattern with point intensity determined by Z . In this way, a
186 spatial correlation function is obtained to compare and evaluate the existing dependences
187 between the ant point pattern and the derived point pattern determined by Z .

188 Let us now replace Z (random fields for weed data) by a point pattern and consider the
189 correlation between two point patterns. So if the random field Z is positive (as it is in our case),
190 we can assume this function as the intensity field function of a Cox process (a family of point
191 processes driven by a random point intensity; see for instance Stoyan et al. 1995), and then

192 generate point realizations based on this point intensity. To obtain the resulting random field Z
 193 from the n field weed samples, we used an ordinary kriging approach based on the global
 194 variogram matrix (Isaaks and Srivastava 1989). Notice that other spatial procedures can be
 195 considered to obtain this random field Z (see for instance, Cressie 1993). Now Z is derived
 196 from values $Z_i = Z(y_i)$ at the points y_i in a grid B (i.e. the prediction values after ordinary
 197 kriging). Note that Z_i can be multiplied by a scaling factor if necessary. Moreover, assuming
 198 that for each cell c_i centred at point location y_i the random field value is constant and equal
 199 to Z_i , we can generate point realizations based on this grid. Now points are located at random
 200 over B and accepted only if $U \leq Z_i / \max(Z_i)$, where $U \sim U(0,1)$, i.e. a uniform random
 201 number. Therefore, areas with large values of Z_i (high-intensity values) are expected to have
 202 greater numbers of points than areas with small values of Z_i , and so on. This procedure will
 203 generate a point pattern based on the intensity function Z_i . After that, label 1 was assigned to
 204 the original point pattern of ant nests and label 2 to the resulting Cox pattern based on Z_i ,
 205 thereby resulting in a bivariate point pattern. Then, summary statistics involving a bivariate
 206 point pattern can be used to evaluate the dependences of both point patterns. Here, we used the
 207 *partial* or *cross-pair correlation* function $g_{12}(r)$ (Illian et al. 2008), for a given inter-point
 208 distance $r > 0$ to evaluate this spatial structure. This correlation function is a bivariate
 209 derivation of the pair correlation function to study the spatial dependences of point classes for
 210 bivariate point patterns. This function indicates point-type inhibition when $g_{12}(r) < 1$,
 211 $g_{12}(r) = 1$ is the Poisson case (i.e. point-types are independently distributed from each other),
 212 while $g_{12}(r) > 1$ implies point-type clustering. An estimator function for this function can be
 213 defined (Illian et al. 2008) as

214

215

$$\hat{g}_{12}(r) = \frac{1}{2\pi\hat{\lambda}_1\hat{\lambda}_2|A|} \sum_{x_1 \in \phi_1, x_2 \in \phi_2} \frac{\kappa(\|x_1 - x_2\| - r)}{e(x_1, \|x_1 - x_2\|)}, \quad (2)$$

216

217 where φ_1 and $\hat{\lambda}_1$ are the point pattern and the point intensity of the point class 1 (say),
218 respectively, for a given inter-point distance r . For the Epanechnikov kernel function, we chose
219 the bandwidth to be equal to $c/\sqrt{\hat{\lambda}}$, where typically $c = 0.1-0.2$ (here $c = 0.2$), as
220 suggested by Stoyan and Stoyan (1994).

221 In order to choose the variogram model that provides the best goodness of fit, we used a
222 cross-validation procedure based on the standardized prediction residuals (Cressie 1993, page
223 102). The spherical and exponential parametric models provided the best mathematical fit for
224 the empirical variograms (see also Table 1). Given that both models provide similar
225 parametrizations, we finally considered the spherical model to be in concordance with similar
226 studies carried out in the same geographic region in which the spherical model also provided the
227 best goodness of fit for similar datasets (Izquierdo et al. 2009a and b). Therefore, this model
228 was considered to provide a valid parametric representation for the ordinary kriging procedures.
229 All the geostatistical and point processes procedures have been computed using the GeoR and
230 the Spatstat statistical packages, respectively, for the R statistical environment (R Development
231 Core Team, 2007).

232

233 *Testing for spatial independence for (bivariate) point patterns*

234 For each kind of spatial correlation function, we tested for spatial independence following a
235 Monte Carlo approach based on the random simulation of (marked) point patterns from the null
236 hypothesis (Poisson). We simulated 999 (bivariate) point patterns under the null hypothesis of
237 spatial independence, and for each one, an estimator of one of the correlation functions defined
238 above was obtained. These set of functions were then compared with the resulting estimator of
239 this correlation function for the point pattern under analysis. Under this test, we rejected the null
240 hypothesis (spatial independence) if the resulting estimator of this correlation function lay
241 outside the 25th largest and/or smallest envelope values obtained from the set of simulated
242 functions with an exact significant level of $\alpha = 2 \times 25 / (999 + 1) = 0.05$. Tests for each

243 (bivariate) point pattern considered here are defined as follows. For the point pattern of ant nets
244 we tested against spatial point independence based on the random simulation of Poisson point
245 configurations (see for instance, Stoyan and Stoyan 1994). Whilst, under the bivariate point
246 patterns (i.e. two point classes i and j) we considered a *random labelling* approach (see, Illian
247 et al. 2008).

248

249 Table 1 around here

250

251 **Results**

252

253 The total number of weed species was 12 and *Papaver rhoeas* L. and *Bromus diandrus* Roth
254 were the most abundant species (Table 2). The number of species per sampling unit ranged from
255 0 to 4.

256

Table 2 around here

257

258 In total, 237 (948 nests/ha) nests were identified and the nest size class two was by far the most
259 abundant in the experimental area (Table 3).

260

261

Table 3 around here

262

263 *Are the locations of ant nests spatially correlated?*

264 Figures 1a and 1b show the spatial positions of ant nests for the five size classes and the related
265 bivariate point pattern assuming only two size classes, namely small (classes 1 and 2) and large
266 (classes 3, 4 and 5) classes, respectively. This size classification is chosen since it provides a
267 reasonable number of points for each class, 185 small nests and 52 large nests, and distinguishes
268 between nests with a single entrance (classes 1 and 2) and nests with more than one entrance
269 (classes 3, 4 and 5). Visual inspection of these point patterns does not provide much information
270 about the spatial dependence of these two point patterns. The resulting pair correlation function

271 (1) for the point pattern of ant nests is shown in Figure 1c together with their respective 25th
272 largest and smallest envelope values based on 999 Poisson point randomizations. This suggests
273 an inhibitory structure for short inter-nest distances of less than 1 m.

274

275 *How are small and large nests related to each other in space?*

276 Similarly, when analysing the spatial configuration of ant nests assuming small and large nest
277 sizes via the resulting cross-pair correlation function (2) (Figure 1d), we reject the null
278 hypothesis of independence and accept that small and large nests are spatially correlated. In
279 particular, this indicates repulsion between nest classes, i.e. large nests (say) are unlikely to be
280 surrounded by small classes at short inter-event distances (<2 m).

281

282 Figure 1 around here

283

284 *Does the presence of ant nests affect weed richness and coverage assuming point process*
285 *correlation functions?*

286 Figures 2 shows the resulting prediction maps $Z(y_i)$ based on an ordinary kriging approach
287 for weed richness and weed cover, together with the spatial locations of the two nest size
288 classes. To perform these ordinary krigings we considered a spherical variogram model for the
289 two empirical variograms (i.e. weed richness and cover) (see Table 4 for the parameter values),
290 based on 96 sampling points, which is an enough number of points to obtain reliable empirical
291 variograms. Once again, visual inspection of these figures does not highlight any apparent
292 spatial structure between ant nests and weed spatial configurations, so the comparison of
293 summary statistics associated with these spatial structures is clearly necessary if we are to detect
294 spatial correlations. Notice that resulting weed richness and cover random fields are visually
295 very similar, thereby suggesting that areas with large number of weed species are also areas
296 with large weed coverage.

297

298

Table 4 around here

299

300

301

302

303

304

305

306

307

308

309

310

311

312

Discussion

313

314

315

316

317

318

319

320

321

322

323

324

325

Figure 3 around here

Let us now consider the spatial correlation between nest locations and the weed random fields based on the cross-pair correlation function (2). Figure 3 shows the resulting cross-pair correlation for ant nest locations (large and small sizes) and the Cox point patterns for the weed random fields, highlighting that ant nest locations and weed richness are negatively correlated for inter-event distances of less than 8 m. This finding suggests that for short inter-event distances high intensities of ant nests results in low weed richness. Note that this result is more evident for large nest sizes than for small ones (see Figure 3c). Moreover, the resulting cross-pair correlations for nest locations and weed cover indicate that these variables are spatially uncorrelated regardless of the nest size (Figure 3d, e and f).

To analyse the spatial dependences between the distribution of ant nests and the spatial configuration of weeds, we used spatial statistical tools derived from point process theory. In particular, we compared the two spatial configurations by assuming two different point patterns. We did so by replacing the weed random fields by a related point pattern, and analysing it with the ant point pattern.

Our results suggest that, in general, areas with a high density of large ant nests are areas with low weed richness. In direct contrast, small nest classes do not apparently affect the resulting structure of weed richness. Our results also suggest that ant nest density does not affect too much weed coverage. Moreover, when analysing the spatial configuration of ant nests we found that small and large nest classes are also negatively correlated, indicating that large nests (say) are unlikely to be surrounded by small classes at short inter-event distances. This spatial inhibition of nests can probably be explained by the killing of smaller colonies by workers

326 belonging to large colonies or by the lower probability of nest initiation success in the
327 proximities of long-established colonies (Hölldobler 1981; Rytí and Case 1992), as pointed out
328 by previous research in cereal fields in NE Spain (Blanco-Moreno et al. 2014). This fact,
329 together with the results obtained in the analysis of the spatial interaction between weed random
330 fields and ant point patterns, suggests that weeds were able to survive in zones with small nests,
331 areas with probably lower ant pressure, and areas where large nests were not found. Seed
332 predation pressure in areas with small ant nests is lower than that in areas with larger nests,
333 because in these areas there are fewer workers and less foraging activity (Crist and Macmahon
334 1992). So, in areas with small nests it is expected that there will be more weed cover than in
335 areas with large nests. Therefore, the presence of large nests apparently regulates the richness
336 and cover of weeds, limiting them to areas with smaller ant nests.

337 There are several factors that could explain ant nest distribution and weed distribution.
338 Among those extrinsic, soil characteristics should be one of the main factors. In this sense
339 however, one study carried out in the same area (Baraibar et al. 2011) showed that none of the
340 studied soil properties could explain ant nest densities in the studied fields. The appointed paper
341 did not perform a spatial analysis relating both variables, but it already highlighted that soil
342 could not be an important factor explaining ant nest distribution. That research and another one
343 in the same study area (Blanco-Moreno et al. 2014), elucidated that other factors not considered,
344 such as seed availability, intraspecific competition or the distribution of landing sites of
345 founding queens, may play an additional role in determining ant density and spatial variability.
346 Anyway, the apparent correlation between ant nests and weed richness found here could be just
347 because large nests occupy a large space, of at least 1 m in diameter, where nest entrances are
348 kept free of plants (Torra, pers. observ.).

349 Regarding the weed cover, some reasons could partially explain its uncorrelation with
350 the spatial arrangement of harvester ant nests. By far, the most abundant and regularly
351 distributed species were *B. diandrus* and *P. rhoeas*. *P. rhoeas* has a very short exposure time to
352 ants on the soil surface because small-sized seeds have a faster seed burial (Westerman et al.
353 2003). This fact, together with its highly persistent seeds, would allow the presence of an

354 important seedbank, which could buffer the regulation exerted by harvester ants on its
355 abundance. In the case of *B. diandrus*, this species is less preferred by harvester ants than other
356 weed species (Westerman et al. 2012).

357 We conclude that large nests of *M. barbarus* can have a bigger impact on weed spatial
358 configurations than small nests. Therefore, preserving and enhancing regular ant nest
359 distributions, especially those of large nests, would have a major negative impact on weed
360 survival, and simultaneously improve weed control measures. Management strategies to
361 promote this effect are desirable, but further research is required to understand the factors
362 affecting ant nest distribution in cereal fields. For example, long-term no-tillage systems in
363 dryland cereal fields would promote bigger nests and higher nest densities compared with tilled
364 fields (Baraibar et al. 2011) or irrigated fields (Baraibar et al. 2009). This research only
365 considered one cereal field. Once the spatial dependencies between weeds and harvester ants are
366 possible to study, the findings of this research should be corroborated in more cereal fields in
367 the study area. Moreover, understanding how management factors affect these spatial
368 interdependencies would be key for improving weed control. Finally, a future research line can
369 be the modelling of such structures, such as ant nests as a Cox process with weed parameters as
370 a covariate. A such work may open up new and promising research lines.

371

372 **Acknowledgements**

373

374 We wish to thank the funding of research by the Ministry of Education and Science of Spain
375 (projects AGL 2007-60828 and AGL 2010-22084-C02-01).

376

377 **References**

378

379 Azcárate FM, Kovacs E, Peco B (2007) Microclimatic conditions regulate surface activity in
380 harvester ants *Messor barbarus*. J Insect Behav 20:315-329.

381 Baraibar B, Westerman PR, Carrión E, Recasens J (2009) Effects of tillage and irrigation in
382 cereal fields on weed seed removal by seed predators. *J Appl Ecol* 46:380-387.

383 Baraibar B, Torra J, Westerman PR (2011) Harvester ant (*Messor barbarus* (L.)) density as
384 related to soil properties, topography and management in semi-arid cereals. *Appl Soil Ecol*
385 51:60-65.

386 Barroso J, Fernández-Quintanilla C, Ruiz D, Hernáiz P, Rew LJ (2004) Spatial stability of
387 *Avena sterilis* ssp. *ludoviciana* populations under annual applications of low rates of
388 imazamethabenz. *Weed Res* 44:178-186.

389 Barroso J, Navarrete L, Sánchez del Arco MJ, Fernández-Quintanilla C, Lutman PJW, Perry
390 NH, Hull RI (2006) Dispersal of *Avena fatua* and *Avena sterilis* patches by natural
391 dissemination, soil tillage and combine harvesters. *Weed Res* 46:118-128.

392 Blanco-Moreno JM, Westerman PR, Atanackovic V, Torra J (2014) The spatial distribution of
393 nests of harvester ants *Messor barbarus* (L.) in dryland cereals. *Insect Soc* 22:145-152.

394 Blanco-Moreno JM, Chamorro L, Sans FX (2006) Spatial and temporal patterns of *Lolium*
395 *rigidum*–*Avena sterilis* mixed populations in a cereal field. *Weed Res* 46:207-218.

396 Blanco-Moreno JM, Sans FX, Chamorro L, Masalles RM, Recasens J (2004) Spatial
397 distribution of *Lolium rigidum* seedlings following seed dispersal by combine harvesters.
398 *Weed Res* 44:375-387.

399 Burton MG, Mortensen DA, Lindquist JL (2006) Effect of cultivation and within-field
400 differences in soil conditions on feral *Helianthus annuus* growth in ridge-tillage maize. *Soil*
401 *Till Res* 88:8-15.

402 Colbach N, Forcella F, Johnson GA (2000) Spatial and temporal stability of weed populations
403 over five years. *Weed Sci* 48:366–377.

404 Comas C (2009) Modelling forest regeneration strategies through the development of a spatio-
405 temporal growth interaction model. *Stoch Environ Res Risk Assess* 23:1089-1102.

406 Comas C, Mateu J (2011) On the Takacs-Fiksel estimation method for forest field observations.
407 *Stoch Environ Res Risk Assess* 25:287-300.

408 Crist TO, Macmahon JA (1992) Harvester ant foraging and shrub-steppe seeds: interactions of
409 seed resources and seed use. *Ecology* 73:1768-1779.

410 Cressie N (1993) *Statistics for Spatial Data*. John Wiley and Sons, New York, USA.

411 Di Virgilio N, Monti A, Venturi G (2007) Spatial variability of switchgrass (*Panicum virgatum*
412 L.) yield as related to soil parameters in a small field. *Field Crop Res* 101:232–239.

413 Díaz M (1991) Spatial patterns of granivorous ant nest abundance and nest site selection in
414 agricultural landscapes of Central Spain. *Insect Soc* 38:351-363.

415 Díaz M (1992) Spatial and temporal patterns of granivorous ant seed predation in patchy cereal
416 crop areas of central Spain. *Oecologia* 91:561-568.

417 Dicke D, Gerhards R, Büchse A, Hurlle K (2007) Modeling spatial and temporal dynamics of
418 *Chenopodium album* L. under the influence of site-specific weed control. *Crop Prot*
419 26:206-211.

420 Dieleman JA, Mortensen DA (1999) Characterizing the spatial pattern of *Abutilon theophrasti*
421 seedling patches. *Weed Res* 39:455-467.

422 Dieleman JA, Mortensen DA, Buhler DD, Ferguson RB (2000) Identifying associations among
423 site properties and weed species abundance. II. Hypothesis generation. *Weed Sci* 48:576-
424 587.

425 Diggle PJ (2003) *Statistical Analysis of Spatial Point Patterns*. Hodder Arnold, London, UK.

426 Ford ED (1975) Competition and stand structure in some even-aged monocultures. *J Ecol*
427 63:311–333.

428 Harkness RD, Isham V (1983) A Bivariate Spatial Point Pattern of Ants' Nests. *J Appl Stat*
429 3:293-303.

430 Heijting S, Van der Werf W, Kropff MJ (2009) Seed dispersal by forage harvester and rigid-tine
431 cultivator in maize. *Weed Res* 49:153-163.

432 Hölldobler B (1981) Foraging and spatiotemporal territories in the honey ant *Myrmecocystus*
433 *mimicus wheeler* (*Hymenoptera: Formicidae*). *Behav Ecol Sociobiol* 9:301-314.

434 Illian J, Penttinen A, Stoyan H, Stoyan D (2008) *Statistical analysis and modelling of spatial*
435 *point patterns*. Wiley, New York, USA.

436 Isaaks EH, Srivastava RM (1989) An Introduction to Applied Geostatistics. Oxford University
437 Press, New York, USA.

438 Izquierdo J, Blanco-Moreno JM, Chamorro L, González-Andújar JL, Sans FX (2009a) Spatial
439 distribution of weed diversity within a cereal field. *Agron Sustain Dev* 29:491-496.

440 Izquierdo J, Blanco-Moreno JM, Chamorro L, Recasens J, Sans FX (2009b) Spatial Distribution
441 and Temporal Stability of Prostrate Knotweed (*Polygonum aviculare*) and Corn Poppy
442 (*Papaver rhoeas*) Seed Bank in a Cereal Field. *Weed Sci* 57:505-511.

443 Law R, Illian J, Burslem DFRP, Gratzler G, Gunatilleke CVS, Gunatilleke IAUN (2009)
444 Ecological information from spatial patterns of plants: insights from point process theory. *J*
445 *Ecol* 97:616-628.

446 Nicolai N, Feagin RA, Smeins FE (2010) Spatial Patterns of Grass Seedling Recruitment Imply
447 Predation and Facilitation by Harvester Ants. *Environ Entomol* 39:127-133.

448 R Development Core Team (2007) R: A Language and Environment for Statistical Computing.
449 R Foundation for Statistical Computing, Vienna. Available at: <http://www.R-project.org>.

450 Ripley BD (1976) The second-order analysis of stationary point processes. *J Appl Probab*
451 13:255-266.

452 Ryti RT, Case TJ (1992) The role of neighborhood competition in the spacing and diversity of
453 ant communities. *Am Nat* 139:355-374.

454 Stoyan D, Stoyan H (1994) Fractals, Random Shapes and Point Fields: Methods of Geometrical
455 Statistics. Wiley, Chichester, UK.

456 Stoyan D, Kendall WS, Mecke J (1995) Stochastic Geometry and its Applications. John Wiley
457 and Sons, New York, USA.

458 Stoyan D, Penttinen A (2000) Recent applications of point process methods in forestry statistics.
459 *Stat Sci* 15:61-78.

460 Tanner CJ, Keller L (2012) Nest distribution varies with dispersal method and familiarity-
461 mediated aggression for two sympatric ants. *Anim Behav* 84:1151-1158.

462 Torra J, Atanackovic V, Blanco-Moreno JM, Royo-Esnal A, Westerman PR (2015) Effect of
463 patch size on seed removal by harvester ants. *Weed Res.* (in press).

464 Wackernagel H (1998) Multivariate geostatistics. Springer, Berlin, Germany.

465 Westerman PR, Wes JS, Kropff MJ, Van der Werf W (2003) Annual losses of weed seeds due
466 to predation in organic cereal fields. *J Appl Ecol* 40:824-836.

467 Westerman PR, Atanackovic V, Royo-Esnal A, Torra J (2012) Differential weed seed removal
468 in dryland cereals. *Arthropod-Plant Inte* 6:591-599.

469 Wiegand T, Kissling WD, Cipriotti PA, Aguiar MNR (2006) Extending point pattern analysis
470 for objects of finite size and irregular shape. *J Ecol* 94:825-837.

471 Wiernasz DC, Cole BJ (1995) Spatial Distribution of *Pogonomyrmex occidentalis*: Recruitment,
472 Mortality and Overdispersion. *J Anim Ecol* 64:519-527.

473 Williams II MM, Mortensen DA, Marx DB (2002) Within-field soil heterogeneity effects on
474 herbicide-mediated crop injury and weed biomass. *Weed Sci* 49:798-805.

475 Woolcock JL, Cousens RA (2000) Mathematical analysis of factors affecting the rate of spread
476 of patches of annual weeds in an arable field. *Weed Sci* 48:27-34.

477

478

479

480

481

482

483

484

485

486

487

488

489

490

491

492
493
494
495
496
497
498
499
500
501
502
503
504
505
506
507
508
509
510
511
512
513
514
515
516

Table 1 Values of a cross-validation procedure based on the standardized prediction residuals for two variogram parametrization initially considered; smaller values indicates better goodness of fit for the model under analysis (Cressie, 1993)

	Weed richness	Weed cover
Spherical	0.00108	0.00002
Exponential	0.00127	-0.00009

517

518 **Table 2** Weeds species found in a sampled area of 50 x 50 m in May 2011 after herbicide
519 spraying in a no-till cereal field in Bellmunt d'Urgell, Spain.

Species	Frequency (n° of sampling units)	Mean percentage coverage ±SE per sampling unit
<i>Bromus diandrus</i>	63	7.2 ± 1.2
<i>Papaver rhoeas</i>	17	4.6 ± 0.7
<i>Veronica hederifolia</i>	7	3.4 ± 0.5
<i>Fumaria densiflora</i>	9	2.7 ± 0.5
<i>Fumaria officinalis</i>	1	5.0
<i>Avena sterilis</i> ssp. <i>ludoviciana</i>	1	1.0
<i>Anacyclus clavatus</i>	3	0.5 ± 0.0
<i>Galium aparine</i>	1	1.0
<i>Galium parisiense</i>	2	0.3 ± 0.0
<i>Lolium rigidum</i>	1	1.0
<i>Herniaria hirsuta</i>	1	0.1
<i>Sonchus oleraceus</i>	1	0.1

520

521

522

523

524

525

526

527

528

529

530

531

532 **Table 3** Abundances of harvester ant nests in an area of 50 x 50 m in August 2011 for five
533 different nest sizes in a no-till cereal field in Bellmunt d'Urgell, Spain.

Nest size class*	Number
1	37
2	148
3	37
4	9
5	6

534 * Subjective scale of nest size from 1 (smallest) to 5 (largest); see Material and Methods.

535

536

537

538

539

540

541

542

543

544

545

546

547

548

549

550

551

552

553

554 **Table 4** Estimated variogram parameter values obtained for weed richness and cover empirical
555 variograms under a spherical variogram model.

	Nugget	Sill	Range
Weed richness	0.083	0.077	20.001
Weed cover	0.699	0.293	13.350

556

557

558

559

560

561

562

563

564

565

566

567

568

569

570

571

572

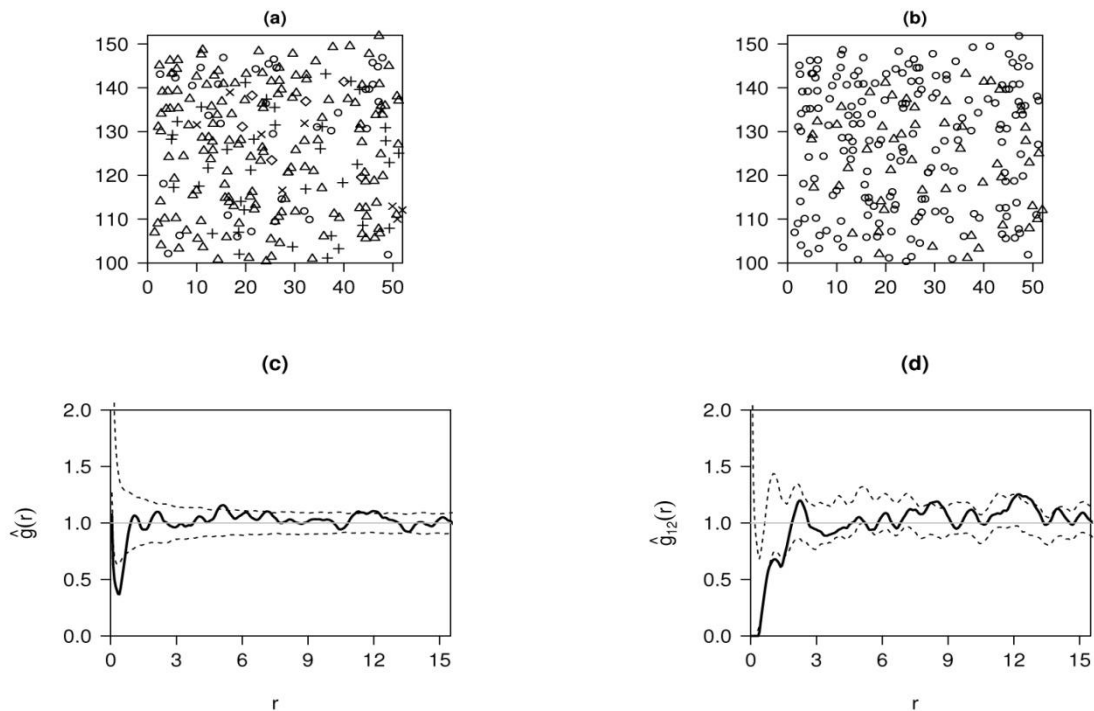
573

574

575

576

577



579

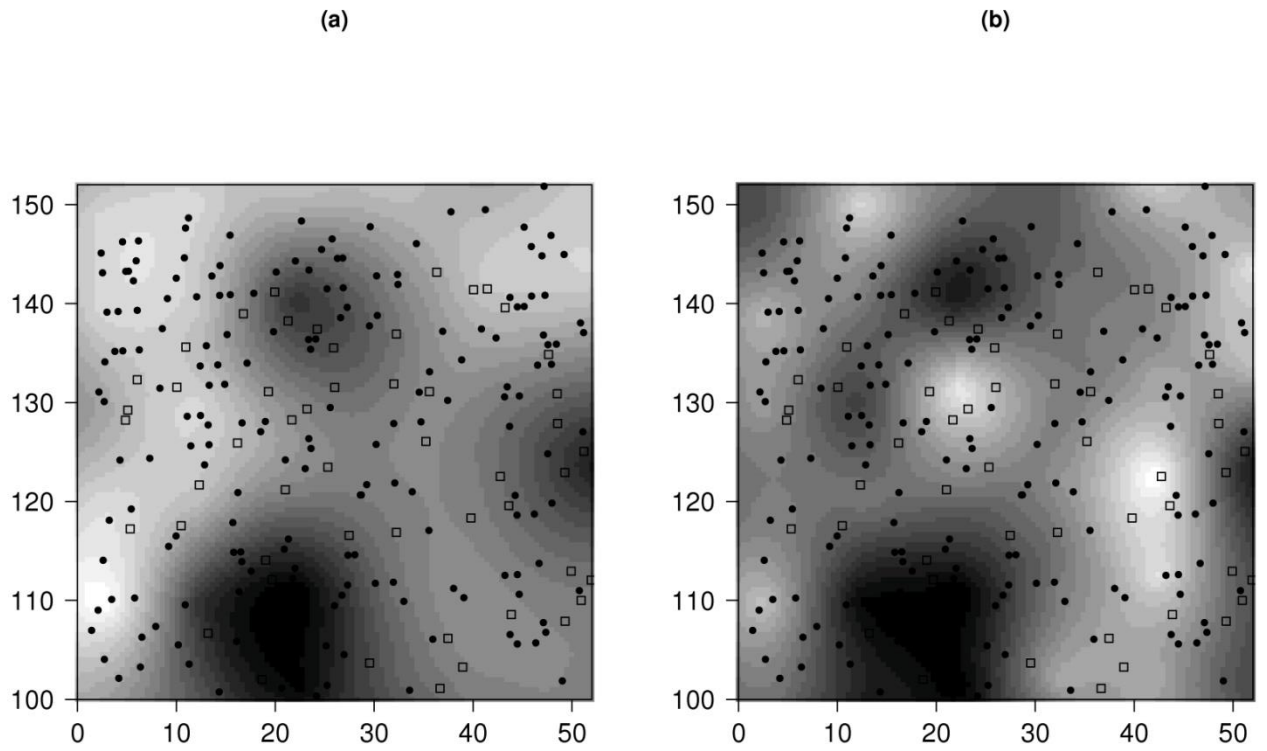
580 **Fig. 1** (a) Point patterns of ant nest positions for five size classes (x and y axes are the nest
 581 positions coordinates): class 1 (circle, smallest class), class 2 (triangle), class 3 (cross), class 4
 582 (multiplication sign), and class 5 (diamond). (b) The related bivariate point pattern assuming
 583 only two size classes: small (circle, classes 1 and 2), and large (triangle, classes 3, 4 and 5) sizes
 584 in a cereal field in Bellmunt d'Urgell, Spain. (c) Resulting estimator of the pair correlation
 585 function (see equation (1)) for all the ant nest positions along with the resulting fifth largest and
 586 smallest envelope values based on 199 Poisson point randomizations (dashed lines). (d)
 587 Resulting estimator of the cross-pair correlation function (see equation (2)) for the ant nest
 588 bivariate point pattern together with the resulting fifth largest and smallest envelope values
 589 based on 999 random labelled (i.e. independent) bivariate point configurations (dashed lines).

590

591

592

593



595

596 **Fig. 2** Resulting maps $Z(y_i)$ based on an ordinary kriging approach for weed richness (a) and

597 cover (b), together with spatial locations of the two nest size classes, large (square) and small

598 (bullet).

599

600

601

602

603

604

605

606

607

608

609

610

611

612

613

614

615

616

617

618

619

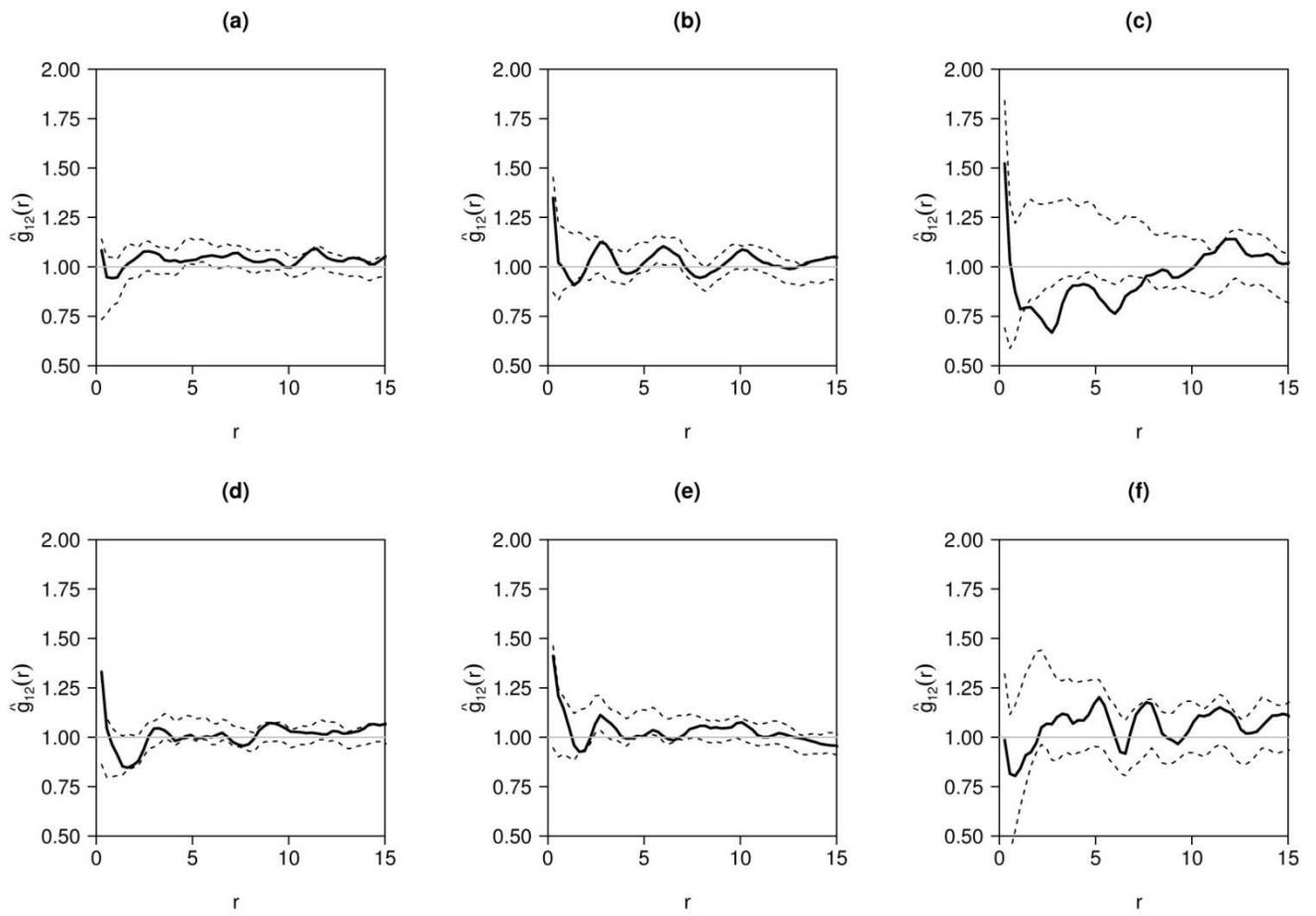
620

621

622

623

624



625

626

627

628

629

Fig. 3 Resulting estimator of the cross-pair correlation function (see equation (2)) for all the ant nest locations (a) and (d), small nest locations (b) and (e), and large nest locations (c) and (f), and the Cox point patterns of weed richness (top row) and weed cover (bottom row), together with the resulting fifth largest and smallest envelope values based on 999 random labelled (i.e. independent) bivariate point configurations (dashed lines).